Published source: Plasma Sources Sci. Technol. 20 (2011) 055002 (7 pages)

Rectification effect of gradient antiparallel magnetic fields on electron conduction in a gas under a radio-frequency electric field

Hirotake Sugawara, Tsuyoshi Osaga and Hiromori Yamamoto

Division of Electronics for Informatics, Graduate School of Information Science and Technology, Hokkaido University, Sapporo 060-0814, Japan

E-mail: sugawara@ist.hokudai.ac.jp

Abstract. Electron transport in CF_4 under linearly gradient antiparallel magnetic fields was analysed in order to investigate the fundamental properties of magnetic neutral loop discharge plasmas used for material processing. The electron motion was simulated by a Monte Carlo method under a radio-frequency (rf) electric field applied perpendicularly to both the directions of the magnetic field and its gradient. Two typical electron motions, meandering in a weak magnetic field and gyration in a strong magnetic field, were observed with particular directionalities. The meandering electrons drifted forward on average similarly to those under a dc electric field. The gyration induced an electron drift towards the inverse direction. The direction of electron flux was dependent not only on the rf phase but also on the distance from the magnetically neutral midplane between the antiparallel magnetic fields. The electron conduction path formed along the midplane had a structure consisting of forward and inverse lanes. A peculiar result was that the direction of local electron flux was always forward in the strong magnetic field whereas the drift of gyrating electrons was towards the inverse direction. This seemingly paradoxical result can appear in the presence of the density gradient of the electron distribution.

PACS numbers: 52.20.-j Elementary processes in plasma, 52.25.Fi Transport properties

Published source: Plasma Sources Sci. Technol. 20 (2011) 055002 (7 pages)

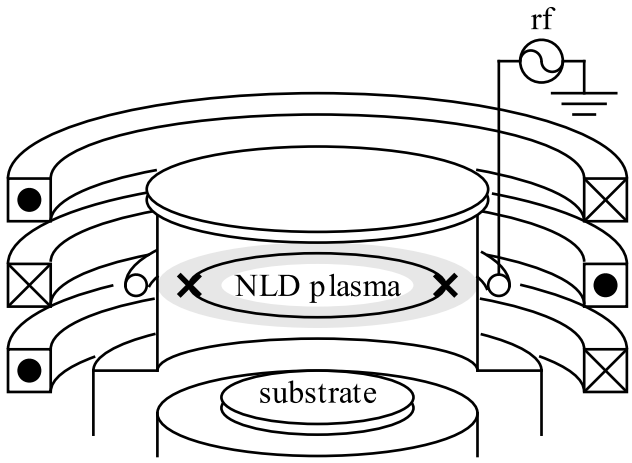

Figure 1. Schematic of a NLD plasma reactor. The loop with X's in the chamber represents the positions of zero magnetic field.

1. Introduction

A magnetic neutral loop discharge (NLD) plasma is a kind of inductively coupled plasma used for material processing in semiconductor fabrication. Its high plasma densities 10^{16}–10^{17} m^{-3} at low gas pressures 0.1–1.0 Pa (Tsuboi *et al* 1995, 1997, O'Connell *et al* 2007) are suitable for anisotropic etching.

The NLD plasma is generated along a ring of a zero magnetic field named the neutral loop (NL). The NL is formed by superposing magnetic fields induced by coaxial coils surrounding the plasma chamber as shown in figure 1 (Uchida 1994, Uchida and Hamaguchi 2008). The magnetic field around the NL has, as a result, a quadrupole structure. Therefore, analysis of the electron motion in the quadrupole magnetic field is effective in order to understand how NLD plasmas are driven.

Some simulations have shown that the electron motion in quadrupole magnetic field is quite complicated (see, e.g., Sakoda *et al* (2001), Okraku-Yirenkyi *et al* (2001), Vural and Brinkmann (2007) and Sugawara *et al* (2010)). Thus, analyses of the essential electron behaviour have often been performed in simplified antiparallel magnetic fields since the quadrupole magnetic field consists of two pairs of antiparallel magnetic fields. Such analyses have revealed fundamental properties of NLD plasmas. Yoshida *et al*

Published source: Plasma Sources Sci. Technol. 20 (2011) 055002 (7 pages)

(1998) analysed electron meandering in such antiparallel magnetic fields under a radio-frequency (rf) electric field. The meandering was understood as a primary process for electrons to receive energy from the electric field. Recently, Sugawara and Sakai (2008) reported a rectification effect of the antiparallel magnetic fields under dc electric fields. Depending on the sign of the electric field applied perpendicularly to both the magnetic field and its gradient, the behaviour of an electron swarm became convergent (conductive) or divergent (resistive). It is adequately considered that some key processes governing NLD plasmas, such as the power deposition from the rf antenna and the conduction of the loop current along the NL, proceed under the influence of this rectification effect.

In this paper, we analyse the electron motion in antiparallel magnetic fields under an rf electric field. We report that the electron conduction path has a structure consisting of forward and inverse lanes under the rectification effect of the antiparallel magnetic fields.

2. Simulation model and conditions

2.1. Electric and magnetic fields

We consider the electron motion in a boundary-free space. The electric and magnetic fields (the $\boldsymbol{E}$ and $\boldsymbol{B}$ fields) were defined in a rectangular coordinate system (x, y, z) as follows:

$$\boldsymbol{E} = (E_x, E_y, E_z) = (0, E_0 \sin 2\pi f t, 0), \tag{1}$$

$$\boldsymbol{B} = (B_x, B_y, B_z) = (0, 0, \beta x), \tag{2}$$

where the $\boldsymbol{E}$ field is uniform all over the space, and $\beta = \mathrm{d}B_z/\mathrm{d}x$ is a constant (see figure 2). The parameters to determine the $\boldsymbol{E}$ and $\boldsymbol{B}$ fields were set as $\beta = 0.25$, 0.50 and 1.00 mT cm^{-1}, $E_0 = -5.0$ V cm^{-1}, and $f = 13.56$ MHz in the simulation.

Linearly gradient antiparallel $\boldsymbol{B}$ fields can be formed by two equal parallel current slabs (Uchida 1998, and Sugawara and Sakai 2008). Similar field configurations for

Published source: Plasma Sources Sci. Technol. 20 (2011) 055002 (7 pages)

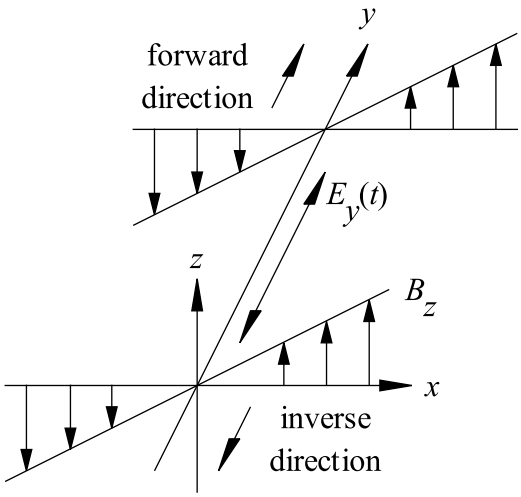

Figure 2. Configuration of the $\boldsymbol{E}$ and $\boldsymbol{B}$ fields. $\boldsymbol{B} = (B_x, B_y, B_z) = (0, 0, \beta x)$, $\beta = \mathrm{d}B_z/\mathrm{d}x = \text{const}$, and $\boldsymbol{E} = (E_x, E_y, E_z) = (0, E_0 \sin 2\pi f t, 0)$. The forward and inverse directions are determined by the rectification effect of the antiparallel $\boldsymbol{B}$ fields on the electron transport.

simulations have been adopted also in Asakura *et al* (1997) and Yoshida *et al* (1998). The $\boldsymbol{B}$ field defined here models one of the two pairs of antiparallel components of the quadrupole $\boldsymbol{B}$ field near the NL of an NLD plasma. The linearity of the gradient $\boldsymbol{B}$ field near the NL was seen in a calculation result by Gans *et al* (2007).

The yz-plane is the magnetically neutral midplane between the antiparallel $\boldsymbol{B}$ fields. The electron conduction path is formed along the y-axis. Here, the $+y$- and $-y$-directions are, respectively, recognized as the forward and inverse directions for the electron transport under the rectification effect of the antiparallel $\boldsymbol{B}$ fields (Sugawara and Sakai 2008). The electrons flying in the $+y$-direction turn inwards to weaker $\boldsymbol{B}$ field under the action of the Lorentz force. This allows electron acceleration towards the $+y$-direction when $E_y < 0$. On the other hand, those flying in the $-y$-direction turn outwards to stronger $\boldsymbol{B}$ field. Electrons gyrate and thus do not drift along the $\boldsymbol{E}$ field when $E_y > 0$. The field configuration is convergent (conductive) for electrons when $E_y < 0$, and is divergent (resistive) when $E_y > 0$. Under an ac $\boldsymbol{E}$ field, the conductive and resistive modes alternate every half a period.

Published source: Plasma Sources Sci. Technol. 20 (2011) 055002 (7 pages)

2.2. Monte Carlo method

The electron motion in the $\boldsymbol{E}$ and $\boldsymbol{B}$ fields was simulated by a Monte Carlo method. The initial electrons were released from the origin with velocities chosen at random form a Maxwellian distribution with a mean energy of 1 eV. CF_4, an etching gas, was chosen as the ambient gas. The gas molecule number density was assumed to be 1.77×10^{14} cm^{-3}, which corresponds to 0.67 Pa at 0°C. The time-saving scheme for judgement of the occurrence of electron–molecule collisions (Sugawara *et al* 2007) was adopted. The set of the electron collision cross sections of CF_4 was taken from Kurihara *et al* (2000). Using the same set of cross sections, Dujko *et al* (2005, 2006) calculated primary electron transport parameters in CF_4 under uniform crossed $\boldsymbol{E}$ and $\boldsymbol{B}$ fields. These results are informative as comprehensive reference data.

The loci of electron flight were calculated using the Runge–Kutta fourth order method. The time step Δt of the locus calculation was chosen to be 3.69 ps, which is 1/20 000 of the rf period $T = 1/f = 73.7$ ns, so that Δt is sufficiently small relative to the cyclotron period dealt with in the present simulation. This Δt value is about 1/1000 of the cyclotron period even at a relatively large value of $|\boldsymbol{B}| = 10.0$ mT, which appears at $x = \pm 10.0$ cm in case of $\beta = 1.00$ mT cm^{-1}. The distance of a flight during Δt is so short that one could treat the $\boldsymbol{B}$ field to be locally uniform within the distance. However, the Runge–Kutta method takes account of the position-dependent variation of the $\boldsymbol{B}$ field in its own calculation scheme.

The electrons were traced for 100 rf periods (7.375 μs), during which the electrons reached their periodical steady state. The number of electrons sampled at the end of the simulation was more than 10^6. The spatial distribution of electrons was sampled with a resolution of $\Delta x = 1$ mm every sampling interval of $T/20$. In order to suppress the statistical fluctuation in the phase-resolved observation, the sampled data were averaged among those of the same rf phase over the last 10 rf periods.

Published source: Plasma Sources Sci. Technol. 20 (2011) 055002 (7 pages)

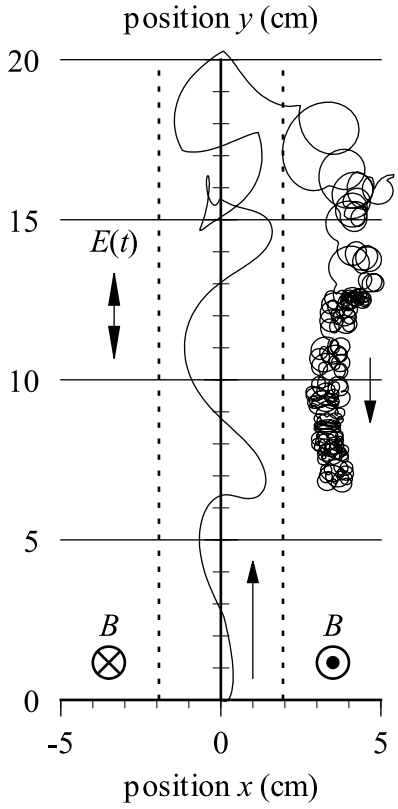

Figure 3. Electron meandering in weak $\boldsymbol{B}$ field and gyration in strong $\boldsymbol{B}$ field. The locus shows a flight for 50 rf periods at $\beta = 0.50$ mT cm^{-1}. The broken lines represent the x-positions at which $|\boldsymbol{B}| = 2B_{\mathrm{ECR}}$. The meandering was towards the $+y$-direction on average, and the drift of gyrating electron was towards the $-y$-direction.

3. Results and discussion

3.1. Single electron motion

Figure 3 shows a typical electron locus in the antiparallel $\boldsymbol{B}$ fields under the rf $\boldsymbol{E}$ field. Two characteristic motions are observed; meandering in the weak $\boldsymbol{B}$ field near $x = 0$ and gyration in the strong $\boldsymbol{B}$ field far from $x = 0$.

The meandering is understood as the process of electron energy gain since the electrons can respond to the alternating $\boldsymbol{E}$ field in the weak $\boldsymbol{B}$ field. However, for the rectification effect of the antiparallel $\boldsymbol{B}$ fields, the meandering electrons drifted to the $+y$-direction, i.e. the direction of $\boldsymbol{B} \times \nabla|\boldsymbol{B}|$, on average. The direction of this drift was

Published source: Plasma Sources Sci. Technol. 20 (2011) 055002 (7 pages)

irrespective of the initial phase of the $\boldsymbol{E}$ field. The drift towards the $+y$-direction during the meandering was unchanged even in the case of $E_0 = +5.0$ V cm^{-1}. The drift of meandering electron was seen also in early investigations by Uchida (1998) and Yoshida *et al* (1998), but its specific directionality was not focused on at that time.

This rectification effect would appear in a practical NLD plasma as a difference of the plasma impedance along the NL or the plasma power between the former and latter halves of an rf period. O'Connell *et al* (2008) reported phase-resolved rf responses of optical emission from a Ne NLD plasma, in which the emission waveform was asymmetric for the two halves of an rf period whereas that was symmetric when no $\boldsymbol{B}$ field was applied. This result suggests the appearance of the rectification effect. In order to clarify the relation between cause and effect, further realistic modelling of the NLD plasma would be necessary. This issue is left for future investigations.

It seems that the gyration occurred mainly in the region where $|\boldsymbol{B}| > 2B_{\mathrm{ECR}}$. Here, B_{ECR} is the strength of the rf-resonant magnetic field. Its value, $B_{\mathrm{ECR}} = 0.484$ mT at $f = 13.56$ MHz, is derived from the condition of electron cyclotron resonance $2\pi f = eB_{\mathrm{ECR}}/m$, where e and m are the electronic charge and mass.

The gyration frequency was dependent on x through $B_z = \beta x$ and was not always synchronous with f. The total electron collision frequency ν was about 2.5×10^7 s^{-1}, 3.0×10^7 s^{-1} and 3.6×10^7 s^{-1} at $\beta = 1.00$ mT cm^{-1}, 0.50 mT cm^{-1} and 0.25 mT cm^{-1}, respectively. A condition $\omega > \nu$, in which the electron transport is in magnetic-field-controlled regime (Dujko *et al* 2005), was satisfied for $|x| > 0.14$ cm, 0.34 cm and 0.82 cm, respectively. Here, $\omega = eB/m = e\beta x/m$ is the cyclotron angular frequency at x.

The gyrating electron drifted towards the $-y$-direction. This direction agrees with that of the grad-B drift, i.e. the direction of $-\boldsymbol{B} \times \nabla|\boldsymbol{B}|$. However, the time-averaged drift velocity of the gyrating electron was 1–2 orders of magnitude greater than the grad-B drift velocity estimated in the absence of the $\boldsymbol{E}$ field. It is considered that the drift of the gyrating electron occurred in the same manner as the grad-B drift, but its

Published source: Plasma Sources Sci. Technol. 20 (2011) 055002 (7 pages)

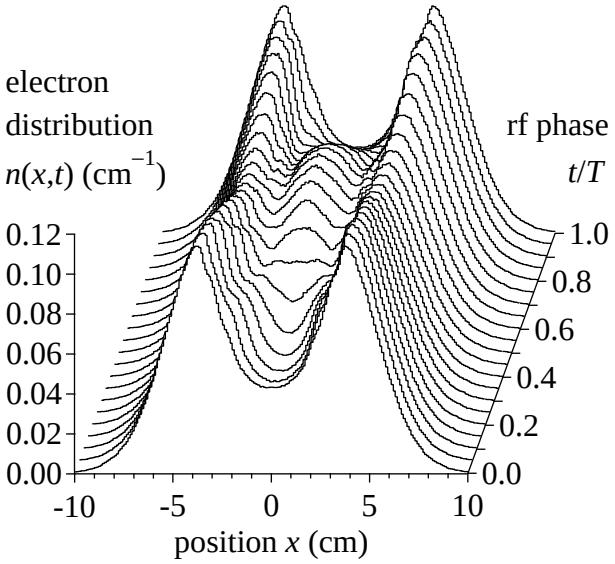

Figure 4. Lateral electron distribution $n(x,t)$ in an rf period T at $\beta = 0.50$ mT cm^{-1}.

velocity was enhanced by the rf $\boldsymbol{E}$ field. Compared with the results under dc $\boldsymbol{E}$ fields by Sugawara and Sakai (2008), the present drift of gyrating electron towards the $-y$-direction is particular to the rf $\boldsymbol{E}$ field. Gyration was observed also under dc $\boldsymbol{E}$ fields in the divergent configuration, but the accompanying drift was outwards, i.e. towards the direction of $\boldsymbol{E} \times \boldsymbol{B}$.

3.2. Lateral electron distribution

Figure 4 shows the temporal variation of the lateral electron distribution $n(x,t)$ at $\beta = 0.50$ mT cm^{-1} in an rf period T. It is characteristic that $n(x,t)$ has two peaks unlike Gaussian distributions obtained under dc $\boldsymbol{E}$ field as shown afterward. The gyration in the regions of $|\boldsymbol{B}| > 2B_{\mathrm{ECR}}$ prolonged the electron residence time there, that formed the peaks. The two peaks moved inwards during $0 \leq t \leq T/2$ and outwards during $T/2 \leq t \leq T$ responding to the alternating $\boldsymbol{E}$ field. The direction of this motion corresponds to that of the $\boldsymbol{E} \times \boldsymbol{B}$ drift in the convergent and divergent configurations.

Figure 5 shows the time average of the normalized lateral electron distributions,

Published source: Plasma Sources Sci. Technol. 20 (2011) 055002 (7 pages)

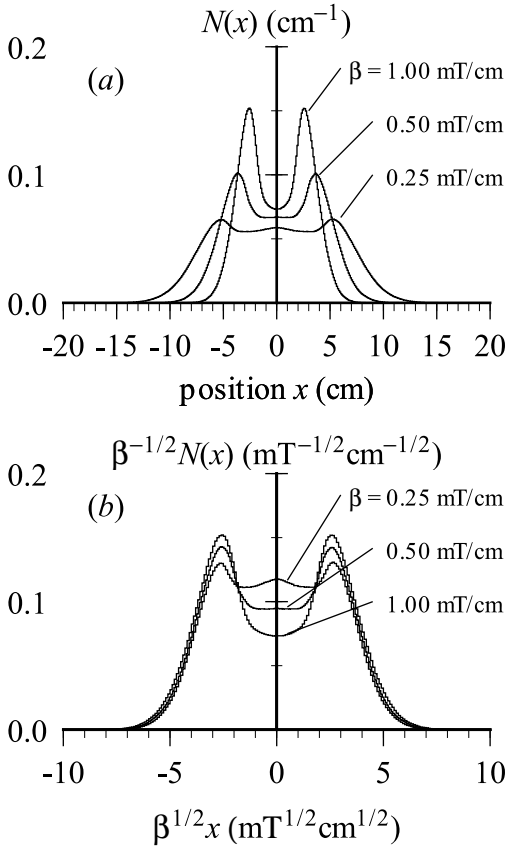

Figure 5. Time-averaged lateral electron distributions $N(x)$ in rf $\boldsymbol{E}$ field (a) and their aspect ratio-modified forms (b).

$N(x)$, under the rf $\boldsymbol{E}$ field:

$$N(x) = \frac{1}{T}\int_0^T \frac{n(x,t)}{\int_{-\infty}^{\infty} n(x,t)\mathrm{d}x}\mathrm{d}t. \tag{3}$$

For a comparison, those under a dc $\boldsymbol{E}$ field ($E_y = -5.0$ V cm^{-1}, convergent configuration) at the same β values are presented in figure 6. The breadth of $N(x)$ under the rf $\boldsymbol{E}$ field was wider than under the dc $\boldsymbol{E}$ field because the field configuration in the rf $\boldsymbol{E}$ field was divergent for half an rf period.

$N(x)$ shrank towards $x = 0$ with increasing β. Sugawara (2008) reported that $N(x)$ under a dc $\boldsymbol{E}$ field was Gaussian with a standard deviation $\sigma \propto 1/\sqrt{\beta}$. A similar dependence of $N(x)$ on β was also seen in those under the rf $\boldsymbol{E}$ field. Figures 5(b) and 6(b), respectively, show the aspect ratio-modified forms of $N(x)$ under the rf and dc $\boldsymbol{E}$ fields; their horizontal and vertical scales were multiplied by $\sqrt{\beta}$ and $1/\sqrt{\beta}$, respectively.

Published source: Plasma Sources Sci. Technol. 20 (2011) 055002 (7 pages)

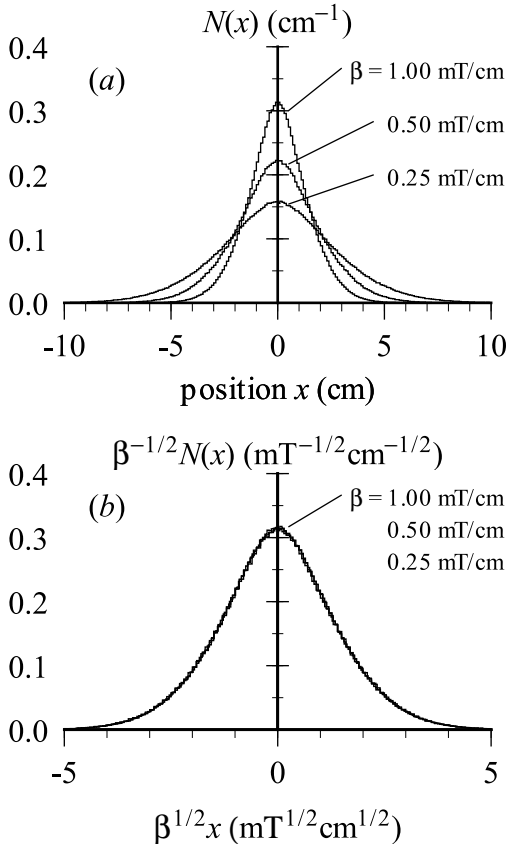

Figure 6. Lateral electron distributions $N(x)$ in dc $\boldsymbol{E}$ field (a) and their aspect ratio-modified forms (overlapping) (b). $N(x)$ is Gaussian and its standard deviation σ has a dependence on β as $\sigma \propto 1/\sqrt{\beta}$.

The aspect ratio-modified $N(x)$ is almost constant under the dc $\boldsymbol{E}$ field (figure 6(b)). Those under the rf $\boldsymbol{E}$ field have common profiles of the peak positions and the decay in the distribution tails (figure 5(b)). On the other hand, the dip between the peaks became deeper with increasing β. This was due to the decrease in the electron multiplication by ionisation. The lateral distribution of the mean electron energy $\varepsilon(x)$ shown in figure 7 indicates that the electron energy gain and the accompanying ionisation in the weak $\boldsymbol{B}$ field near $x = 0$ were suppressed at higher β.

The feature that the breadth of $N(x)$ is inversely proportional to $\sqrt{\beta}$ was also observed in results of another simulation using Ar, performed for a comparison, in the same field configuration. The essential properties of the electron behaviour and the

Published source: Plasma Sources Sci. Technol. 20 (2011) 055002 (7 pages)

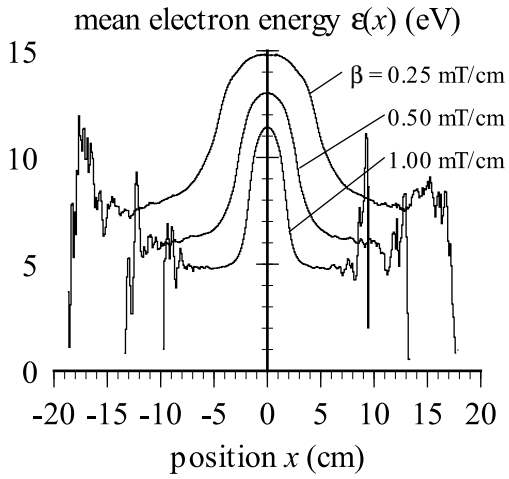

Figure 7. Time-averaged mean electron energy $\varepsilon(x)$ in rf $\boldsymbol{E}$ field. The oscillations at the outer ends are statistical fluctuations.

two-peaked form of $N(x)$ were unchanged. Differences dependent on the characteristics of the gas were that the relaxation in Ar proceeded faster than in CF_4 and that the dip between the peaks of $N(x)$ was shallower in Ar; because ionisation occurred more in Ar than in CF_4, it is considered that the electron multiplication promoted the relaxation and filled the dip.

3.3. Electron flux

Figure 8 shows the temporal variation of the normalized electron flux $\phi(x,t) = W_y(x,t)n(x,t)$ in an rf period, where $W_y(x,t)$ is the y-component of the mean electron velocity at a position x. Since $n(x,t)$ is normalized, the integral of $\phi(x,t)$ over x gives the average electron velocity in the y-direction. The time-averaged electron flux $\Phi(x) = \int_0^T \phi(x,t)\mathrm{d}t/T$ is also shown in figure 9. The electron conduction path had a structure consisting of lanes distinguished by the directionality of the electron transport. The inner, middle and outer lanes can be identified as described below.

The inner lane is the path for the electrons meandering in the weak $\boldsymbol{B}$ field near $x = 0$. The sign of $\phi(x,t)$ alternated as positive and negative responding to the rf $\boldsymbol{E}$ field with a phase delay about 60°, and $\phi(x,t) > 0$ on average (i.e. $\Phi(x) > 0$) for the

Published source: Plasma Sources Sci. Technol. 20 (2011) 055002 (7 pages)

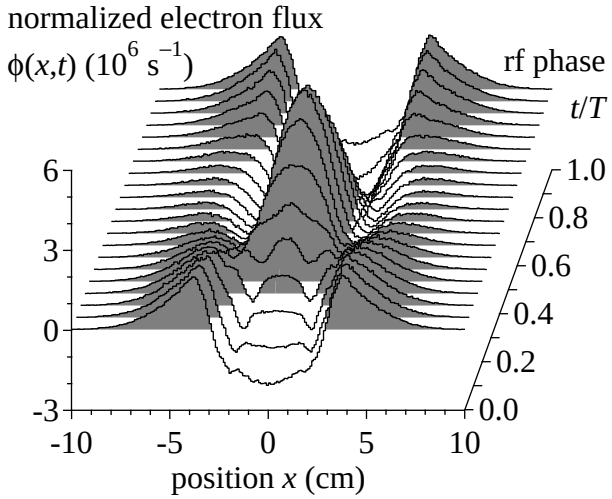

Figure 8. Normalized electron flux distribution $\phi(x,t) = n(x,t)W_y(x,t)$ in an rf period T at $\beta = 0.50$ mT cm^{-1}. The hatching represents $\phi(x,t) > 0$.

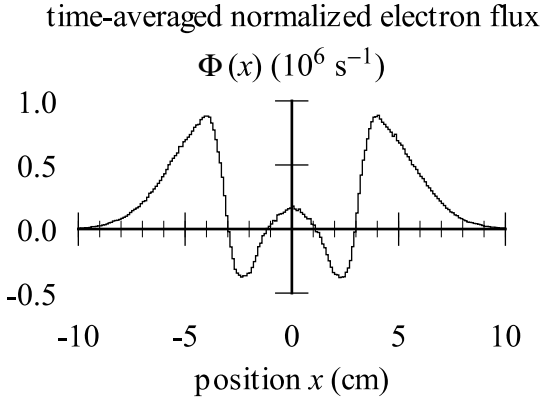

Figure 9. Time-averaged electron flux $\Phi(x) = \int_0^T \phi(x,t)\mathrm{d}t/T$ at $\beta = 0.50$ mT cm^{-1}.

rectification effect of the antiparallel $\boldsymbol{B}$ fields.

The outer lanes are the regions in which $\phi(x,t) > 0$ throughout $0 \leq t \leq T$ and as a result $\Phi(x) > 0$. The outer lanes are located outside of the peaks of $n(x,t)$, where the electron gyration occurs. Here, recall that the drift of gyrating electrons was towards the $-y$-direction. The direction of the flux of electrons was opposite to that of the single electron drift. An interpretation for this seemingly paradoxical result is presented in detail in section 3.4.

Published source: Plasma Sources Sci. Technol. 20 (2011) 055002 (7 pages)

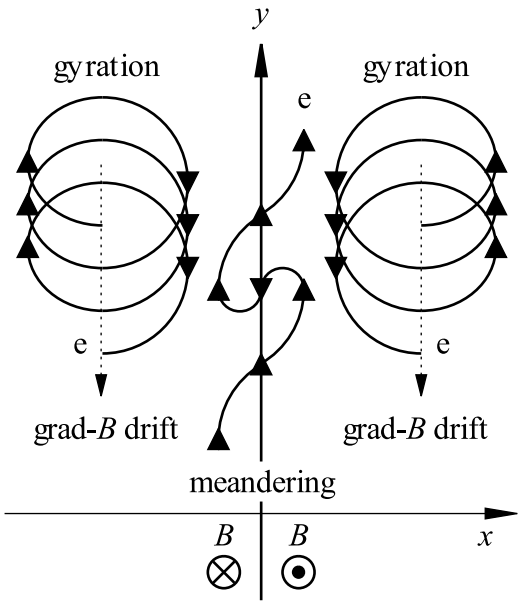

Figure 10. Schematic of single electron motion. The meandering is towards the $+y$-direction and the drift accompanying gyration is towards the $-y$-direction, on average.

The middle lanes are the intermediate regions between the inner and outer lanes. $\Phi(x) < 0$ in the middle lanes was in exchange for $\Phi(x) > 0$ in the outer lanes. This is also explained in section 3.4.

Tsuboi and Ogata (2007) presented an equivalent circuit model to evaluate the power deposition into an Ar NLD plasma. In the model, the NLD plasma was regarded as a ring conductor inductively coupled with an rf antenna. The present finding on the structure of the electron conduction path gives information for an extension of the equivalent circuit model.

3.4. Sign of electron flux of gyrating electrons

Figure 10 shows a schematic of the electron meandering and gyration. Let us analyse the y-component of the electron motion in gyration.

First, we consider a single electron gyration. The electron flux observed in the gyration is positive when the electron is on the outside of its guiding centre, and is negative when it is on the inside. The entire electron flux of gyrating electrons is

Published source: Plasma Sources Sci. Technol. 20 (2011) 055002 (7 pages)

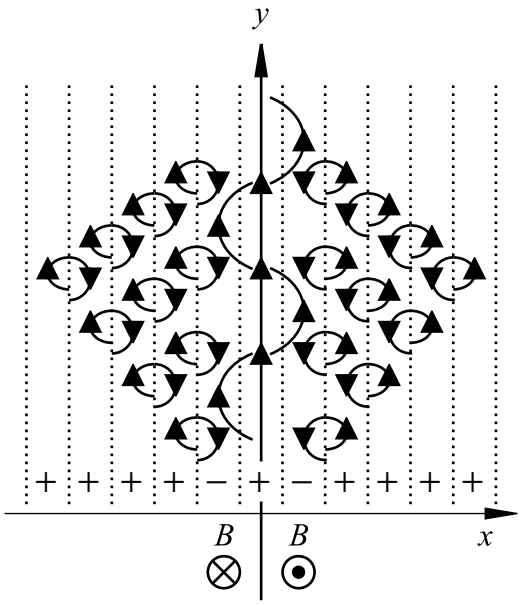

Figure 11. Local value of net electron flux in the presence of the density gradient of electron distribution. The upward and downward arrowheads on the electron loci, respectively, represent the positive and negative contributions to the net electron flux.

negative because they drift towards the $-y$-direction.

Next, we consider gyrating electrons distributed laterally. The electron flux at a position x is the sum of the negative flux of electrons having guiding centres outside of x and the positive flux of those having guiding centres inside of x. Here, this summation is made for such electrons that the distances of the guiding centres from x are shorter than their Larmor radii. The net electron flux at x can be positive when $N(x)$ decreases outwards.

Figure 11 illustrates the summation of the positive and negative fluxes in an $N(x)$ having a density gradient. The positive flux exceeds the negative locally in the region where $N(x)$ decreases outwards. This was observed in $\phi(x,t)$ in figure 8 as $\phi(x,t) > 0$ in the x region outside of the peaks of $n(x,t)$.

The appearance of the negative flux, which represents the drift of gyrating electrons towards the $-y$-direction, was localized in the region inside of the $n(x,t)$ peaks. The middle lanes were formed by this localization. The negative flux in the middle lanes

was in part cancelled by the positive flux of the meandering electrons, but the negative contribution exceeded to result in $\Phi(x) < 0$.

4. Conclusions

Electron transport in antiparallel gradient magnetic fields under rf electric field was simulated using a Monte Carlo method as an investigation for fundamental properties of NLD plasmas. Meandering in a weak magnetic field and gyration in a strong magnetic field were observed, and they showed directional drifts under the rectification effect of the antiparallel magnetic fields.

The electron conduction path formed along the magnetically neutral midplane between the antiparallel magnetic fields had a structure consisting of three kinds of lanes; i.e. the inner, middle and outer lanes. They were distinguished by the directionality of the electron flux. The sign of the time-averaged electron flux was positive in the inner and outer lanes and negative in the middle lanes.

In the inner lane, meandering electrons moved back and forth responding to the alternating electric field, and the time-averaged electron flux was positive because of the same rectification effect of the antiparallel magnetic fields as previously discussed for the dc electric field. In the outer lanes, where the electron gyration occurred, the local electron flux was always positive while the entire electron flux concerned with the drift of gyrating electrons was negative. This was because the lateral electron distribution had a density gradient decreasing outwards. The appearance of the negative flux of the gyrating electrons was concentrated in a region inside of the two peaks of the lateral electron distribution, that formed the middle lanes.

The breadth of the lateral electron distribution, which represents the thickness of the electron conduction path, was inversely proportional to the square root of the gradient of the magnetic field. This dependence was common for dc and rf electric fields.

In order to simulate practical responses of the NLD plasma, e.g. power deposition and optical emission, we have to take account of many interrelated factors such as the

space charge field, the dynamics of charged and excited species, the boundary condition and the interaction with the external circuit. In a framework to analyse the NLD plasma by establishing an overall model, the present findings on the directional electron conduction will help us to obtain appropriate insight about the macroscopic plasma responses consisting of the microscopic electron behaviour.

Acknowledgments

The authors wish to thank Prof A Murayama of Hokkaido University for valuable comment and kind encouragement. This work was supported by Grant-in-Aid No. 22540500 from the Japan Society for the Promotion of Science and by ULVAC Inc.

References

Asakura H, Takemura K, Yoshida Z and Uchida T 1997 *Japan. J. Appl. Phys.* **36** 4493–6

Dujko S, Raspopović Z M and Petrović Z Lj 2005 *J. Phys. D: Appl. Phys.* **38** 2952–66

Dujko S, White R D, Ness K F, Petrović Z Lj and Robson R E 2006 *J. Phys. D: Appl. Phys.* **39** 4788–98

Gans T, Crintea D L, O'Connell D and Czarnetzki U 2007 *J. Phys. D: Appl. Phys.* **40** 4508–14

Kurihara M, Petrović Z Lj and Makabe T 2000 *J. Phys. D: Appl. Phys.* **33** 2146–53

O'Connell D, Crintea D L, Gans T and Czarnetzki U 2007 *Plasma Sources Sci. Technol.* **16** 543–8

O'Connell D, Gans T, Crintea D L, Czarnetzki U and Sadeghi N 2008 *Plasma Sources Sci. Technol.* **17** 024022

Okraku-Yirenkyi Y, Sung Y-M, Otsubo M, Honda C and Sakoda T 2001 *J. Vac. Sci. Technol.* A **19** 2590–5

Sakoda T, Okraku-Yirenkyi Y, Sung Y M, Otsubo M and Honda C 2001 *Japan. J. Appl. Phys.* **40** 6607–12

Sugawara H 2008 *Bulletin Am. Phys. Soc.* **53** 24

Sugawara H, Mori N, Sakai Y and Suda Y 2007 *J. Comp. Phys.* **223** 298–304

Sugawara H, Osaga T, Tsuboi H, Kuwahara K and Ogata S 2010 *Japan. J. Appl. Phys.* **49** 086001

Sugawara H and Sakai Y 2008 *J. Phys. D: Appl. Phys.* **41** 135208

Tsuboi H, Hayashi T and Uchida T 1997 *Japan. J. Appl. Phys.* **36** 6540–4

Tsuboi H, Itoh M, Tanabe M, Hayashi T and Uchida T 1995 *Japan. J. Appl. Phys.* **34** 2476–81

Tsuboi H and Ogata S 2007 *Japan. J. Appl. Phys.* **46** 7475–7

Published source: Plasma Sources Sci. Technol. 20 (2011) 055002 (7 pages)

Uchida T 1994 *Japan. J. Appl. Phys.* **33** L43–4

Uchida T 1998 *J. Vac. Sci. Technol.* A **16** 1529–36

Uchida T and Hamaguchi S 2008 *J. Phys. D: Appl. Phys.* **41** 083001

Vural M and Brinkmann R P 2007 *J. Phys. D: Appl. Phys.* **40** 510–9

Yoshida Z, Asakura H, Kakuno H, Morikawa J, Takenuma K, Takizawa S and Uchida T 1998 *Phys. Rev. Lett.* **81** 2458–61